Journal Name

ARTICLE TYPE

Cite this: DOI: 10.1039/xxxxxxxxxx

Molecular electrometer and binding of cations to phospholipid bilayers†

Andrea Catte,[a‡] Mykhailo Girych,[b] Matti Javanainen,[c,d] Claire Loison,[e] Josef Melcr,[f] Markus S. Miettinen,[g,h] Luca Monticelli,[i] Jukka Määttä,[j] Vasily S. Oganesyan,[a] O. H. Samuli Ollila,[*b] Joona Tynkkynen,[c] and Sergey Vilov,[e]

Received Date
Accepted Date

DOI: 10.1039/xxxxxxxxxx

www.rsc.org/journalname

Despite the vast amount of experimental and theoretical studies on the binding affinity of cations — especially the biologically relevant Na^+ and Ca^{2+} — for phospholipid bilayers, there is no consensus in the literature. Here we show that by interpreting changes in the choline headgroup order parameters according to the 'molecular electrometer' concept [Seelig *et al., Biochemistry*, 1987, **26**, 7535], one can directly compare the ion binding affinities between simulations and experiments. Our findings strongly support the view that in contrast to Ca^{2+} and other multivalent ions, Na^+ and other monovalent ions (except Li^+) do not specifically bind to phosphatidylcholine lipid bilayers at sub-molar concentrations. However, the Na^+ binding affinity was overestimated by several molecular dynamics simulation models, resulting in artificially positively charged bilayers and exaggerated structural effects in the lipid headgroups. While qualitatively correct headgroup order parameter response was observed with Ca^{2+} binding in all the tested models, no model had sufficient quantitative accuracy to interpret the Ca^{2+}:lipid stoichiometry or the induced atomistic resolution structural changes. All scientific contributions to this open collaboration work were made publicly, using `nmrlipids.blogspot.fi` as the main communication platform.

1 Introduction

Due to its high physiological importance — nerve cell signalling being the prime example — interaction of cations with phospholipid membranes has been widely studied via theory, simulations, and experiments. The relative ion binding affinities are generally agreed to follow the Hofmeister series[1–9], however, consensus on the quantitative affinities is currently lacking. Until 1990, the consensus (documented in two extensive reviews[2,3]) was that while multivalent cations interact significantly with phospholipid bilayers, for monovalent cations (with the exception of Li^+) the interactions are weak. This conclusion has since been strengthened by further studies showing that bilayer properties remain unaltered upon the addition of sub-molar concentrations of monovalent salt[4,10,11]. Since 2000, however, another view has emerged, suggesting much stronger interactions between phospholipids and monovalent cations, and strong Na^+ binding in particular[6–9,12–18].

The pre-2000 view has the experimental support that (in contrast to the significant effects caused by any multivalent cations) sub-molar concentrations of NaCl have a negligible effect on phospholipid infrared spectra[4], area per molecule[10], dipole potential[19], lateral diffusion[11], and choline head group order parameters[20]; in addition, the water sorption isotherm of a NaCl–phospholipid system is highly similar to that of a pure NaCl solution — indicating that the ion–lipid interaction is very weak[4].

The post-2000 'strong binding' view rests on experimental and above all ~~simulation~~ simulational findings. At sub-molar NaCl concentrations, the rotational and translational dynamics of membrane-embedded fluorescent probes ~~decrease~~decreased[7,9,12], and atomic force microscopy (AFM) ex-

[a] School of Chemistry, University of East Anglia, Norwich, NR4 7TJ, United Kingdom
[b] Department of Neuroscience and Biomedical Engineering, Aalto University, Espoo, Finland
[c] Tampere University of Technology, Tampere, Finland
[d] University of Helsinki, Helsinki, Finland
[e] Univ Lyon, Université Claude Bernard Lyon 1, CNRS, Institut Lumiére Matiére, F-69622, LYON, France
[f] Institute of Organic Chemistry and Biochemistry, Czech Academy of Sciences, Flemingovo nám. 2, 16610 Prague 6, Czech Republic, Charles University in Prague, Faculty of Mathematics and Physics, Ke Karlovu 3, 121 16 Prague 2, Czech Republic
[g] Fachbereich Physik, Freie Universität Berlin, Berlin, Germany
[h] Max Planck Institute of Colloids and Interfaces, Department of Theory and Bio-Systems, Potsdam, Germany
[i] Institut de Biologie et Chimie des Protéines (IBCP), CNRS UMR 5086, Lyon, France
[j] Aalto University, Espoo, Finland
[*]**Author to whom correspondence may be addressed. E-mail: samuli.ollila@aalto.fi.**

† Electronic Supplementary Information (ESI) available: 5 figures, detailed technical discussion and simulation details. See DOI: 10.1039/b000000x/

‡ The authors are listed in alphabetical order.

periments ~~show~~ showed changes in bilayer hardness[14–18]; in atomistic molecular dynamics (MD) simulations, phospholipid bilayers consistently ~~bind~~ bound Na^+, although the binding strength ~~depends~~ depended on the model used[12,13,21–26].

Some observables have been interpreted in favour of both views. For example, as the effect of monovalent ions (except Li^+) on the phase transition temperature is tiny (compared to the effect of multivalent ions), it was initially interpreted as an indication that only multivalent ions and Li^+ specifically bind to phospholipid bilayers[2]; however, such a small effect in calorimetric measurements was later interpreted to indicate that also Na^+ binds[8,12]. Similarly, the lack of significant positive electrophoretic mobility of phosphatidylcholine (PC) vesicles in the presence of NaCl (again in contrast to multivalent ions and Li^+) suggested weak binding of Na^+[1,8,14,15,27]; however, these data ~~have also been~~ were also explained by a countering effect of the Cl^- ions[22,28]. ~~To~~ Furthermore, to reduce the area per lipid in scattering experiments, molar concentrations of NaCl ~~are~~ were required[10], ~~which indicates~~ indicating weak ion–lipid interaction; in MD simulations, however, already orders of magnitude lower concentrations ~~result~~ resulted in Na^+ binding and a clear reduction of area per lipid[12,23]. Finally, ~~in noninvasive NMR experiments,~~ lipid lateral diffusion ~~is~~ was unaltered by NaCl in noninvasive NMR experiments[11]; however, ~~it is reduced in simulations~~ as it was reduced upon Na^+ binding ~~, which supports interpreting~~ in simulations, the reduced lateral diffusion of fluorescent probes[7,9,12] ~~as favouring~~ has been interpreted to support the post-2000 'strong binding' view.

In this paper, we set out to solve the apparent contradictions between the pre-2000 and post-2000 views. To this end, we employ the 'molecular electrometer' concept, according to which the changes in the C–H order parameters of the α and β carbons in the phospholipid head group (see Fig. 1) can be used to measure the ion affinity ~~to~~ for a PC lipid bilayer[20,29–31]. ~~As~~ As the order parameters can be accurately measured in experiments and directly compared to simulations[20,29–32,33], ~~, employing~~ [33], applying the molecular electrometer as a function of cation concentration allows the comparison of binding affinity between simulations and experiments. In addition to demonstrating the usefulness of this general concept, we show that the response of the α and β order parameters to penetrating cations is qualitatively correct in MD simulations, but that in several models the affinity of Na^+ for PC bilayers is grossly overestimated. Moreover, we show that the accuracy of lipid–Ca^{2+} interactions in current models is not enough for atomistic resolution interpretation of NMR experiments.

This work ~~has been~~ was done as an Open Collaboration at `nmrlipids.blogspot.fi`; all the related files[34] and almost all the simulation data (`https://zenodo.org/collection/user-nmrlipids`) are openly available.

2 Results and Discussion

2.1 Background: Molecular electrometer in experiments

The ~~molecular electrometer concept is based on~~ basis for the molecular electrometer is the experimental observation that binding of any charged objects (~~e.g.~~ ions, peptides, anesthetics, amphihiles) on a PC bilayer interface ~~induces~~ induced systematic changes in the choline ~~β and α segment~~ and β segment C–H order parameters[20,29–31,35–40]. ~~Thus~~[20,29–32,35–40]. Being systematic, these changes ~~can be used to determine~~ could be employed for determining the binding affinities of the charged objects ~~. The~~ in question. Originally the molecular electrometer was ~~originally~~ devised for cations [20,29] [20,29,32], but further experimental quantification with various positively and negatively charged molecules showed that the choline order parameters S^{α}_{CH} and S^{β}_{CH} in general vary linearly with small amount of bound charge per lipid[29–31,35–40]. ~~The~~ Let now $S^i_{CH}(0)$, where i refers to either α or β, denote the order parameter in the absence of bound charge; the empirically observed linear relation ~~can~~ can then be written as[41]

$$\Delta S^i_{CH} = S^i_{CH}(X^{\pm}) = S - S^i_{CH}(0) + \frac{4m_i}{3\chi} = \frac{4m_i}{3\chi} X^{\pm}, \qquad (1)$$

~~where $S^i_{CH}(0)$ is the order parameter in the absence of bound charges~~Here $X^{\pm}$ is the amount of bound charge per lipid, m_i ~~is~~ an empirical constant depending on the valency and position of bound charge, ~~$X^{\pm}$ is the amount of the bound charge per lipid, i refers to either α or β,~~ and the value of the quadrupole coupling constant ~~is~~ $\chi \approx 167$~~kHz. The change in order parameters with respect to a bilayer without bound charges then becomes~~

$$\Delta S^i_{CH} = S^i_{CH}(X^{\pm}) - S^i_{CH}(0) = \frac{4m_i}{3\chi} X^{\pm}.$$

~~For Ca^{2+} binding to POPC bilayer (in the presence of 100 mM NaCl), combination of atomic absorption spectra and ^{2}H NMR experiments gave $m_\alpha = -20.5$ and $m_\beta = -10.0$~~[29]. kHz.

~~The absolute values of order parameters increase for~~ With bound positive charge, the absolute value of the β ~~and decrease for~~ segment order parameter increases and the α segment ~~with bound positive charge~~ order parameter decreases (and *vice versa*

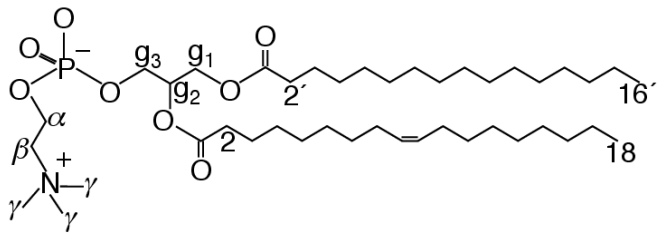

Fig. 1 Chemical structure of 1-palmitoyl-2-oleoylphosphatidylcholine (POPC), and the definition of γ, β, α, g_1, g_2 and g_3 segments.

This journal is © The Royal Society of Chemistry [year]

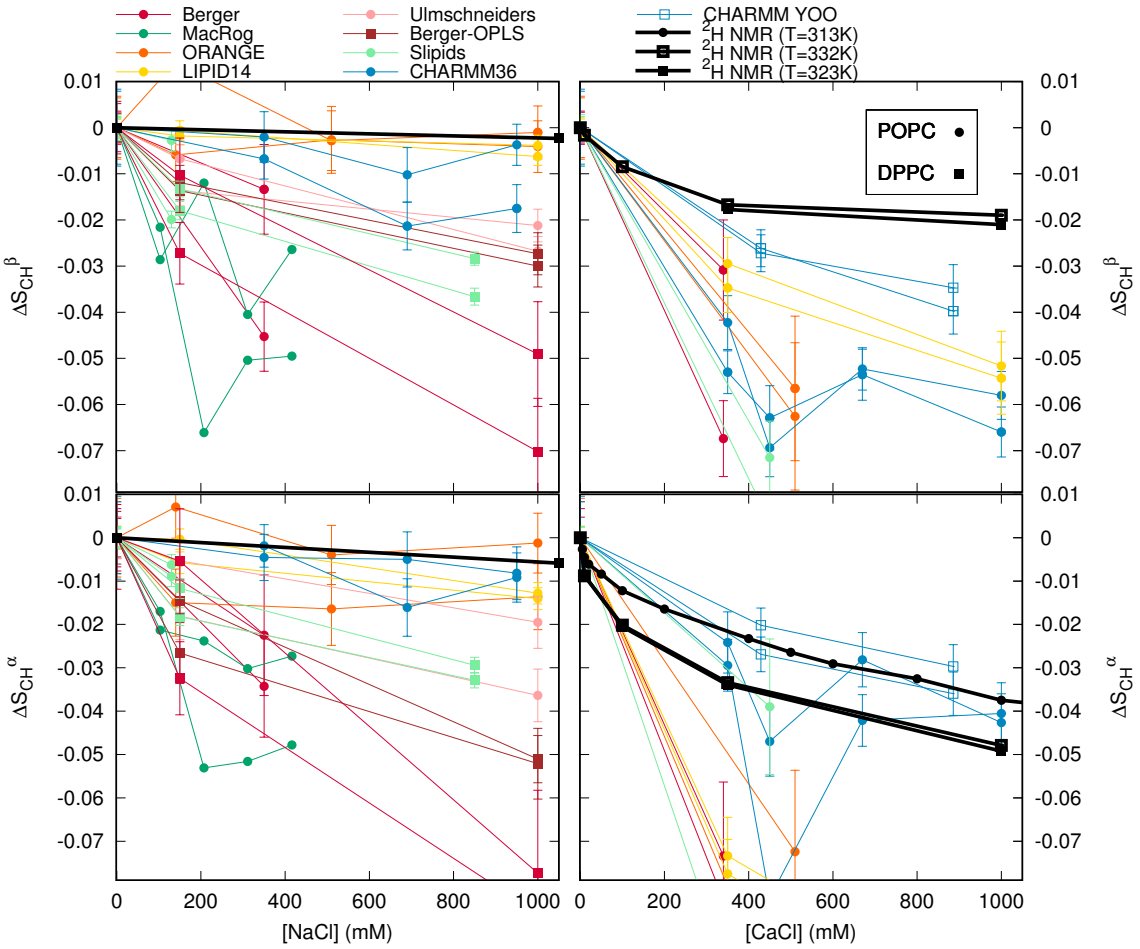

Fig. 2 ~~The order parameter changes for~~ Changes in the PC lipid headgroup β (top row) and α ~~segments as a function of~~ (bottom) segment order parameters in response to NaCl (left column) ~~and~~ or $CaCl_2$ (right~~column~~) salt solution concentration ~~, from~~ increase. Comparison between simulations (Table 1) and experiments ~~[20]~~ (DPPCs from Ref. 20 , POPC ~~with $CaCl_2$~~ from ~~[29]~~ Ref. 29). The signs of the experimental ~~order parameters~~values, ~~taken~~ from experiments without ions [42–44], can be assumed ~~to be~~ unchanged ~~with~~ at these salt concentrations~~represented here~~ [29,33]. ~~It should be noted~~ We stress that none of the models ~~used here~~ reproduces the order parameters without salt within experimental error~~for pure PC bilayer without ions~~, indicating structural inaccuracies ~~with~~ of varying severity in all ~~models~~ of them [45]. Note that the relatively large ~~decrease~~ drop in CHARMM36 ~~with~~ at 450 mM $CaCl_2$ ~~arise~~ arose from more equilibrated binding ~~affinity~~ due to a very long simulation ~~times~~time, see ESI†.

for negative charge~~[20,29–31,35,40])~~ [20,29–32,35,40]. However, as ~~the β carbon order parameter is negative while α carbon order parameter is positive~~ $S^{\beta}_{CH}(0) < 0$ while $S^{\alpha}_{CH}(0) > 0$ [42–44], ~~we can conclude that~~ both ΔS^{β}_{CH} and ΔS^{α}_{CH} in fact decrease with bound positive charge (and increase with bound negative charge). Consequently, values of m_i are negative for bound positive charges; for Ca^{2+} binding to POPC bilayer (in the presence of 100 mM NaCl), combination of atomic absorption spectra and ^{2}H NMR experiments gave $m_{\alpha} = -20.5$ and ~~vice versa. This~~ $m_{\beta} = -10.0$ [29]. This decrease can be rationalised by electrostatically induced ~~changes in~~ tilting of the choline P–N dipole~~tilt~~ [30,31,46], ~~which is~~ [30,31,46] — also seen in simulations [23,24,47,48]. ~~This~~ — and is in line with ~~order parameter decrease~~ the order parameter increase related to the P–N vector tilting more parallel to the membrane plane seen with decreasing hydration levels [45].

~~The quantification of ΔS^{β}_{CH} and~~ Quantification of ΔS^{α}_{CH} ~~with different cations have revealed that $\Delta S^{\beta}_{CH}/\Delta S^{\alpha}_{CH} \approx 0.5$~~ and ΔS^{β}_{CH} for a wide range of different cations (aqueous cations, cationic peptides, cationic anesthetics) has revealed that $\Delta S^{\beta}_{CH}/\Delta S^{\alpha}_{CH} \approx 0.5$ [38,40]. More specifically, the relation $\Delta S^{\beta}_{CH} = 0.43\Delta S^{\alpha}_{CH}$ was found ~~for a DPPC bilayer with~~ to hold for DPPC bilayers at various $CaCl_2$ concentrations [20].

2.2 Molecular electrometer ~~concept~~ in MD simulations

The ~~headgroup order parameter changes as a function of ion concentration in solution from H^2 NMR experiments are shown~~ black curves in Fig. 2 show how the headgroup order parameters for DPPC and POPC bilayers ~~[20,29]~~. change in H^2 NMR experiments as a function of salt solution concentration [20,29]: Only minor changes ~~in order parameters~~ are seen as a function of ~~NaCl in solution, while~~ [NaCl], but the effect of [$CaCl_2$] is an order of magnitude larger. Thus, according to the molecular electrometer~~concept,~~ , the monovalent Na^+ ions have negligible affinity for PC lipid bilayers at concentrations up to 1 M, while binding of Ca^{2+} ions at the same concentration is significant [20,29].

Figure 2 also reports order parameter changes calculated from

MD simulations of DPPC and POPC lipid bilayers as a function of NaCl or $CaCl_2$ initial concentrations in solution (for details of the simulated systems see ~~Tables 1 , ??~~ Table 1 and ESI†). Note that although none of these MD models ~~reproduced~~ reproduces within experimental uncertainty the order parameters for a pure PC bilayer without ions (~~Figure~~ Fig. 2 in Ref. 45), ~~indicating~~ which indicates structural inaccuracies of varying severity in all models[45]. ~~However,~~ , all the models qualitatively reproduce the experimentally observed headgroup order parameter increase with dehydration~~was qualitatively reproduced by all the models [45] , and similarly here~~ [45] . Similarly here (Fig. 2) the presence of cations ~~leads~~ led to the decrease of S_{CH}^{β} ~~and~~ S_{CH}^{α} ~~(Fig. 2)~~and S_{CH}^{β}, in qualitative agreement with experiments. The changes ~~are~~were, however, overestimated by most models~~. According to the electrometer concept this~~ , which according to the molecular electrometer indicates overbinding of cations in most MD ~~simulation models~~simulations.

While ~~electrometer concept~~ the molecular electrometer is well established in experiments (see ~~previous section~~Sec. 2.1 above), it is not *a priori* clear that it works in simulations. The overestimated order parameter decrease could, in principle, arise ~~also from the oversensitivity of choline headgroups on cation binding~~ from an exaggerated response of the choline headgroups to the binding cations, instead of overbinding. ~~Here we analyse~~ Therefore, to evaluate the usability of the molecular electrometer in MD simulations, we analysed the relation between cation binding and choline order parameter decrease in simulations~~in order to evaluate the usability of the electrometer concept in MD simulations~~.

According to the molecular electrometer~~concept,~~ , the order parameter changes are linearly proportional to the amount of bound cations ~~in bilayer~~ (Eq. (2.1)). Figure 3 shows ~~the changes in order parameter as a function of bound charge~~ this proportionality in MD simulations (see ESI† for the definition of bound ions); in keeping with the molecular electrometer, a roughly linear correlation between bound cation charge and order parameter change ~~is~~ was found in all the eight models. Note that quantitative comparison of the proportionality constants (i.e. slopes in Fig. 3) between different models and experimental slopes ($m_\alpha = -20.5$ and $m_\beta = -10.0$ for Ca^{2+} binding in DPPC bilayer in the presence of 100mM NaCl~~in Eq. ??~~ [29]) is not straightforward since the simulation slopes depend on the definition used for bound ions (see ESI†).

~~The~~ We note that the quantitative comparison of order parameter changes in response to bound charge ~~is~~ should be more straightforward for systems with charged amphiphiles fully associated in the bilayer, as the amount of bound charge is then explicitly known in both simulations and experiments. ~~Such comparison between previously published simulation data [49] and experiments [31,50]~~ In such a comparison between experiments [31,50] and previously published Berger-model-based simulations [49] , we could not rule out overestimation of order parameter response to bound cations (~~i.e., slopes m_β and~~ slopes m_α ~~) in a Berger-based model~~ (and m_β), see ESI†~~)~~. This might, in principle, explain the overestimated order parameter response

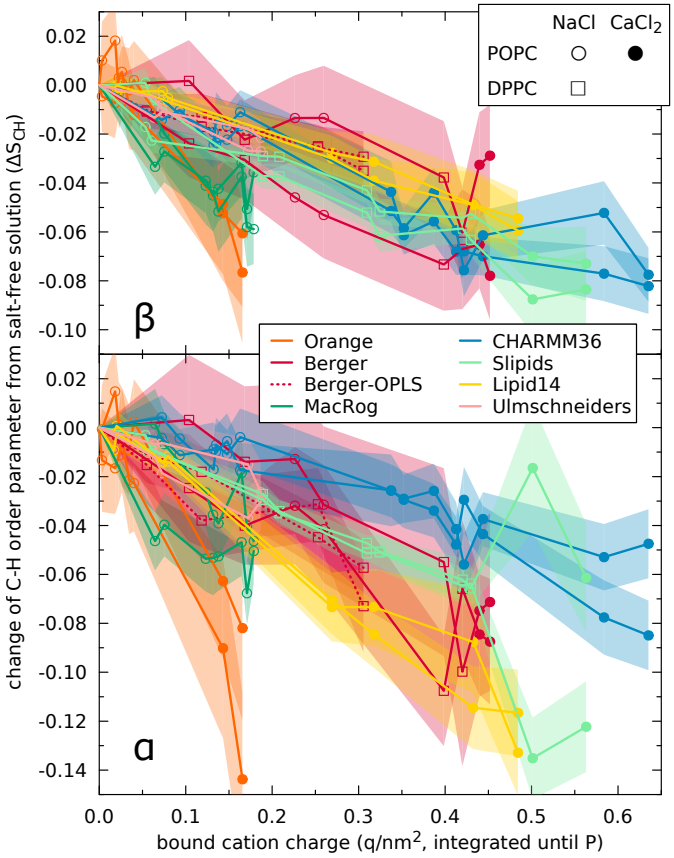

Fig. 3 Change of order parameters (from salt-free solution) of the β and α segments, ΔS_{CH}^{β} and ΔS_{CH}^{α}, ~~shown~~ as a function of bound cation charge. Eight MD simulation models compared; the two lines per model denote to the two hydrogens per carbon. The order parameters as well as the bound charge calculated separately for each leaflet; cations residing between the bilayer centre and the density maximum of Phosphorus considered bound; error bars (shaded) show standard error of mean over lipids.

of the Berger model to $CaCl_2$, but not to NaCl (see discussion in ESI†). Since simulation data with charged amphiphiles ~~from other models is not available , the~~ are not available for other models, an extended comparison with different models is left for further studies.

Figure 3 shows that the decrease ~~on order parameter clearly correlates~~ of order parameters clearly correlated with the amount of bound cations ~~also~~ in simulations. This is also evident from Fig. 4, which shows the Na^+ density profiles of the MD models ordered according to the order parameter change (~~reported~~ in Fig. 2) from the smallest (top) to the largest (bottom). The general trend in the figure is that the Na^+ density peaks are larger for models with larger changes in order parameters, in line with the observed correlation between cation binding and order parameter decrease in Fig. 3. ~~Atom number density profiles along the membrane normal for lipids, Na^+, and Cl^- ions from simulations with different force fields and different NaCl concentrations. The force fields are ordered according to the order parameter changes reported in Fig. 2, from the smallest (top panel) to the largest (bottom panel). The lipid densities are scaled by 100 (united atom) or 200 (all atom model) to improve~~

This journal is © The Royal Society of Chemistry [year]

~~readability.~~

Figure 5 compares the relation between ΔS^{β}_{CH} and ΔS^{α}_{CH} in experiments[20] and ~~different simulation~~ in MD models. Only Lipid14 ~~gives~~ gave $\Delta S^{\beta}_{CH}/\Delta S^{\alpha}_{CH}$ ratio in agreement with the experimental ratio~~. In all the other models~~ ; all other models underestimated the α segment order parameter decrease with bound cations ~~is underestimated~~ with respect to the β ~~order parameter~~ segment decrease.

In conclusion, ~~the~~ a clear correlation between bound cations and order parameter decrease ~~is observed in all the tested~~ was observed for all simulation models. Consequently, the ~~electrometer concept~~ molecular electrometer can be used to compare the cation binding affinity between experiments and simulations. However, we ~~find that the quantitative~~ found that quantitatively the response of α and β segment order parameters to bound cations in simulations ~~do~~ did not generally agree with the experiments~~. The~~ ; e.g., the $\Delta S^{\beta}_{CH}/\Delta S^{\alpha}_{CH}$ ratio ~~agrees~~ agreed with experiments only in the Lipid14 model (Fig. 5). Thus, the observed overestimation of the order parameter changes with ~~cation concentrations may~~salt concentrations could, in principle, arise from overbinding of ~~ions or from too sensitive~~ cations or from an oversensitive lipid headgroup response ~~on bound cation~~ to the bound cations (see also discussion in ESI†). A careful analysis with current lipid models is performed in the next section.

2.3 Cation binding in different simulation models

The order parameter changes (Fig. 2) and density distributions (Fig. 4) ~~demonstrate~~ demonstrated significantly different Na^+ binding affinities in different simulation models. The best agreement with experiments (lowest ΔS^{α}_{CH} and ΔS^{β}_{CH}) ~~is observed for those~~ was observed for the three models (Orange, ~~CHARMM36, and~~ Lipid14, CHARMM36; see Fig. 2) that ~~also predict~~ predicted the lowest Na^+ densities ~~in the membrane proximity~~ near the bilayer (Fig. 4). ~~In all the other tested models ,~~ All the other models clearly overestimated the choline order parameter responses to NaCl ~~are clearly overestimated~~ (Fig. 2) ~~, and~~ — and notably the strength of the overestimation ~~is~~ was clearly linked to the strength of the Na^+ binding affinity (compare Figs. 2 and 4)~~;~~ ~~this~~ , which leads us to conclude that ~~sodium binding affinity is~~ Na^+ binding affinity was overestimated in all these models.

~~In~~ As in the best three models ~~,~~ the order parameter changes with NaCl ~~are~~ were small (< 0.02), ~~so with~~ the achieved statistical accuracy ~~we cannot~~ did not allow us to conclude which of the three ~~has~~ had the most realistic Na^+ binding affinity, especially at physiological NaCl concentrations (~~~150mM~~ 150 mM) relevant for most applications. The overestimated binding in the other models ~~raise questions on~~ raises questions concerning the quality of ~~the~~ predictions from these models when NaCl is present. Especially interactions between charged molecules and ~~lipid~~ the bilayer might be significantly affected by the strong Na^+ binding, ~~as it makes the bilayer effectively positively charged~~which gives the otherwise neutral bilayer an effective positive charge.

Significant Ca^{2+} binding affinity ~~to a phosphatidylcholine bilayer~~ for phosphatidylcholine bilayers at sub-molar concentrations is agreed on in the literature[2,3,20,29], however, several details ~~are yet~~ remain under discussion. Simulations suggest that Ca^{2+} ~~bind~~ binds to lipid carbonyl oxygens with a coordination number of 4.2[13], while interpretation of NMR and scattering experiments suggest that one Ca^{2+} interacts mainly with the choline groups[106–108] of two phospholipid molecules[29]. ~~Simulation~~ A simulation model correctly reproducing the order parameter changes would resolve the discussion by giving atomistic resolution interpretation for the experiments.

As a function of $CaCl_2$ concentration, all models but one (CHARMM36 with ~~recent ion model~~ the recent heptahydrated Ca^{2+} by Yoo et al.[76]) ~~, model overestimate~~ overestimated the order parameter decrease (Fig. 2)~~. According~~ , which according to the molecular electrometer ~~, this indicates overestimated~~ indicates too strong Ca^{2+} binding. ~~This~~ (We note that while this is the most likely scenario for the models ~~where~~ that overestimated changes in both order parameters~~were overestimated, however, in the case of~~ , for $CaCl_2$ ~~we cannot exclude the possibility~~ it is possible also that the headgroup response is oversensitive to bound cations~~(~~, see ESI†~~).~~.) In CHARMM36 with ~~ion model~~ the heptahydrated Ca^{2+} by Yoo et al.[76], ~~ΔS_{CH} is overestimated for β but underestimated for α~~ΔS^{β}_{CH} was overestimated but ΔS^{α}_{CH} underestimated (Fig. 2), in line with ~~Fig. 5 where~~ the $\Delta S^{\beta}_{CH}/\Delta S^{\alpha}_{CH}$ ratio in CHARMM36 ~~is~~ being larger than in experiments ~~. Since~~ (Fig. 5). As we do not know ~~if~~ whether ΔS^{β}_{CH} or ΔS^{α}_{CH} ~~is more realisticin CHARMM36~~was more realistic, we cannot conclude ~~if~~ whether Ca^{2+} binding ~~is~~ was too strong or ~~weak in this simulation model~~too weak in CHARMM36. This could be resolved by comparing ~~CHARMM36 model to the~~ against experimental data with a known amount of bound charge (e.g., ~~experiments with~~ amphiphilic cations[31,50]), however, such simulation data are not currently available.

The ~~ion~~ density distributions with $CaCl_2$ ~~in Fig. 6 show~~ showed significant Ca^{2+} binding in all models (Fig. 6), however, some differences ~~occur~~ occurred in details. The Berger model ~~predicts deeper penetration depth (density maxima close to ±~~predicted deeper penetration (density maximum at ~ 1.8~~ nm) compared to other models (~~density maxima close to ±~~~ 2 ~~nm). The~~ nm); the latter value is probably more realistic ~~since~~ as ^{1}H NMR and neutron scattering data indicate that Ca^{2+} interacts mainly with the choline group[2,106–108]. In CHARMM36 ~~, almost~~ (but not in Slipids) practically all Ca^{2+} ions present in ~~simulation bind in bilayer indicating strongest binding affinity among the tested models. The difference is not as clear in Fig. 2 because α carbon order parameters are the least sensitive to bound charge in CHARMM36~~ the simulation bound the bilayer within 2 μs (Fig. ~~3).~~ 6 and ESI†), which hints that the Ca^{2+} binding affinity of CHARMM36 is among the strongest of these models.

The origin of inaccuracies in lipid–ion interactions and binding affinities ~~in different models~~ is far from clear. Potential candidates ~~could be, for example~~are, e.g., discrepancies in the ion models[109–111], incomplete treatment of electronic polarizability[112], ~~or~~ and inaccuracies in the lipid headgroup description[45].

Considering the ion models, Cordomi et al.[24] showed ~~that~~ the Na^+ binding affinity ~~decreases~~ to decrease when ion radius ~~increases in the model, however, also the models with the largest~~

Table 1 List of MD simulations~~performed in this work~~. The ~~ion~~ salt concentrations ~~are~~ calculated as [~~ion~~salt]=~~(~~$N_{ion} \times_c \times$[water]~~)~~$/N_w$, where [water] = 55.5 M. ~~These~~ ; these correspond the concentrations reported in the experiments by Akutsu et al.[20]. The lipid force fields ~~are~~ named as in our previous work[45].

~~Force field (lipid, ion)~~force field for lipids / ions	lipid	salt	[~~Ion~~salt] ~~mM~~ (mM)	[a] N_l	[b]
Berger-POPC-07[51] / –	POPC	no	0	128	7
Berger-POPC-07[51] ~~,~~/ ffgmx[53]	~~POPC~~ "	NaCl	340 ~~(NaCl)~~	~~128~~ "	7
Berger-POPC-07[51] ~~,~~/ ffgmx[53]	~~POPC~~ "	~~340 (~~$CaCl_2$ ~~) 128~~	~~7157~~ 340	~~0~~ "	~~44~~ 71
Berger-DPPC-97[56] / –	DPPC	no	0	72	2
Berger-DPPC-97[56] ~~,~~/ ffgmx[53]	~~DPPC 150 (NaCl)~~ "	~~72~~ NaCl	~~2880~~ 150	~~8~~ "	
Berger-DPPC-97[56] ~~,~~/ ffgmx[53]	~~DPPC~~ "	"	1000 ~~(NaCl)~~	~~72~~ "	2
BergerOPLS-DPPC-06[60] / –	DPPC	no	0	72	2
BergerOPLS-DPPC-06[60] ~~,~~/ OPLS[62]	~~DPPC 150 (NaCl)~~ "	~~72~~ NaCl	~~2880~~ 150	~~8~~ "	
BergerOPLS-DPPC-06[60] ~~,~~/ OPLS[62]	~~DPPC~~ "	"	1000 ~~(NaCl)~~	~~72~~ "	2
CHARMM36[65] / –	POPC	no	0	~~72~~ 128	~~2242~~ 52
CHARMM36[65] / –	"	"	0	~~303~~ 72	22
CHARMM36[65] ~~,~~/ CHARMM36[68]	~~POPC~~ "	NaCl	350 ~~(NaCl)~~	~~72~~ "	2
CHARMM36[65] ~~,~~/ CHARMM36[68]	~~POPC 690 (NaCl)~~ "	~~72~~ "	~~2085~~ 690	~~26~~ "	
CHARMM36[65] ~~,~~/ CHARMM36[68]	~~POPC~~ "	"	950 ~~(NaCl)~~	~~72~~ "	2
CHARMM36[65] ~~,~~/ CHARMM36	~~POPC~~ "	~~350 (~~$CaCl_2$ ~~)~~	350	128	6
CHARMM36[65] ~~,~~/ CHARMM36	~~POPC~~ "	"	450 ~~($CaCl_2$)~~	200	9
CHARMM36[65] ~~,~~/ CHARMM36	~~POPC~~ "	"	670 ~~($CaCl_2$)~~	128	6
CHARMM36[65] ~~,~~/ CHARMM36	~~POPC~~ "	~~1000 ($CaCl_2$)~~ "	~~128~~ 1000	~~6400~~ "	
CHARMM36[65] ~~,~~/ –	DPPC	no	0	128	80
CHARMM36[65] / Yoo[76]	~~DPPC~~ "	~~430 (~~$CaCl_2$ ~~)~~	~~128~~ 430	~~7760~~ "	~~0~~ 77
CHARMM36[65] ~~,~~/ Yoo[76]	~~DPPC~~ "	~~886 ($CaCl_2$)~~ "	~~128~~ 890	~~7520~~ "	~~0~~ 75
MacRog[77] / –	POPC	no	0	~~288~~ 128	~~14400~~ 64
MacRog[77] / –	"	"	0	~~310~~ 288	144
MacRog[77] ~~,~~/ OPLS[62]	~~POPC~~ "	NaCl	100 ~~(NaCl)~~	~~288~~ "	14
MacRog[77] ~~,~~/ OPLS[62]	~~POPC~~ "	"	210 ~~(NaCl)~~	~~288~~ "	14
MacRog[77] ~~,~~/ OPLS[62]	~~POPC~~ "	"	310 ~~(NaCl)~~	~~288~~ "	14
MacRog[77] ~~,~~/ OPLS[62]	~~POPC~~ "	"	420 ~~(NaCl)~~	~~288~~ "	14
Orange ~~, OPLS[62]~~ / –	POPC	no	0	72	2
Orange ~~,~~/ OPLS[62]	~~POPC~~ "	NaCl	140 ~~(NaCl)~~	~~72~~ "	2
Orange ~~,~~/ OPLS[62]	~~POPC~~ "	"	510 ~~(NaCl)~~	~~72~~ "	2
Orange ~~,~~/ OPLS[62]	~~POPC~~ "	"	1000 ~~(NaCl)~~	~~72~~ "	2
Orange ~~,~~/ OPLS	~~POPC~~ "	~~510 (~~$CaCl_2$ ~~)~~	~~72~~ 510	~~2802~~ "	~~0~~ 28
Slipids[86] [87] / –	~~DPPC~~ POPC	no	0	128	~~3840~~ ~~0~~ 51
Slipids[86] ~~, AMBER[90,91]~~ [87] / AMBER[92]	~~DPPC~~ "	~~150 (NaCl)~~ NaCl	~~600~~ 130	~~18000~~ 200	~~49~~ 90
Slipids[86] ~~, AMBER[90,91] DPPC~~ [87] / AMBER[62]	~~850 (NaCl)~~ "	~~128~~ $CaCl_2$	~~3726~~ 450	~~57~~ "	
~~Slipids[87]~~ Slipids[86] / –	~~POPC~~ DPPC	no	0	128	~~5120~~ 38
Slipids[86] / AMBER[90,91]	"	NaCl	150	~~89~~ 600	180
Slipids[87] ~~, AMBER[92]~~ [86] / AMBER[90,91]	~~POPC~~ "	~~130 (NaCl)~~ "	850	128	37
Slipids[86] / AMBER[90,91]	~~21~~ "	~~0~~ "	~~21~~ 1750	~~310~~ "	36
Slipids[87] ~~, AMBER[62] POPC~~ [86] / AMBER[90,91]	~~450 (CaCl)~~ "	~~200~~ "	~~9000~~ 2570	~~0~~ "	~~73~~ 35
Lipid14[96] ~~, AMBER[62]~~ / –	POPC	no	0	128	5
Lipid14[96] ~~,~~/ AMBER[62]	~~POPC 150 (NaCl)~~ "	~~128~~ NaCl	~~5120~~ 150	~~12~~ "	
Lipid14[96] ~~,~~/ AMBER[62]	~~POPC 1000 (NaCl)~~ "	~~128~~ "	~~5120~~ 1000	~~77~~ "	
Lipid14[96] ~~,~~/ AMBER[62]	~~POPC~~ "	~~350 (~~$CaCl_2$ ~~)~~	~~128~~ 350	~~6400~~ "	~~0~~ 64
Lipid14[96] ~~,~~/ AMBER[62]	~~POPC~~ "	~~1000 ($CaCl_2$)~~ "	~~128~~ 1000	~~6400~~ "	
Ulmschneiders[102] ~~, OPLS[62]~~ / –	POPC	no	0	128	5
Ulmschneiders[102] ~~,~~/ OPLS[62]	~~POPC 150 (NaCl)~~ "	~~128~~ NaCl	~~5120~~ 150	~~12~~ "	
Ulmschneiders[102] ~~,~~/ OPLS[62]	~~POPC 1000 (NaCl)~~ "	~~128~~ "	~~5120~~ 1000	~~77~~ "	

a ~~The number~~ Number of lipid molecules
b ~~The number~~ Number of water molecules
c ~~The number~~ Number of ~~Na^+ molecules~~ $_{Na}$ [d] N_{Ca} [e] N_{Cl} cations
f Simulation temperature
g ~~The total~~ Total simulation time
h Time ~~frames~~ used ~~in the~~ for analysis
i Reference for simulation files
j ~~The number of lipid molecules~~
k ~~The number of water molecules~~
l ~~The number of Na^+ molecules~~

This journal is © The Royal Society of Chemistry [year]

radius show significant binding in DPPC bilayer simulated with is increased; however, in their DPPC bilayer simulations (with the OPLS-AA force field[113]) even the largest Na^+ radii still resulted in significant binding. In our results, the Slipids model gives force field gave essentially similar binding affinity with ion parameters from Refs. 92 and 90,91 (Fig. 4). Further, the compensation of missing electronic polarizability by scaling the ion charge[112,114] reduced Na^+ binding in Berger, BergerOPLS and SlipidsmodelsBerger-OPLS and Slipids, but not enough to be in reach agreement with experiments (ESI†). The charge-scaled Ca^{2+} model[115] slightly reduced binding in CHARMM36, but did not have significant influence on binding in Slipids (ESI†). Significant reduction of The heptahydrated Ca^{2+} binding was observed with ion model ions by Yoo et al[76]. [76] significantly reduced Ca^{2+} binding in CHARMM36 (Fig. 6), however, the CHARMM36 lipid model must be further analysed to fully interpret the results.

On the other hand, also the The lipid models may have also have a significant influence on ion binding behaviour. For example, the same ion model and non-bonded parameters are used in the Orange and BergerOPLS [60] simulationsOrange and Berger-OPLS [60], but while Na^+ ion binding affinity appears realistic in the Orangemodel, it is appeared realistic in Orange, it was significantly overestimated in the BergerOPLS Berger-OPLS (Fig. 4). However, realistic Na^+ binding does not directly relate to automatically imply realistic Ca^{2+} binding (see Orange, Lipid14, and CHARMM36 in Fig. 2) or realistic choline order parameter response to bound charge (see Orange and CHARMM36 in Fig. 5). It should be also also be noted that the low binding affinity of Na^+ in CHARMM36 model is due to the additional repulsion added between (NBFIX [68]) added between the sodium ions and lipid oxygens (NBFIX) [68] (ESI†), and that in the Ca^{2+} model by Yoo et al. [76] the calcium is forced to be solvated solely by water. Altogether, our results indicate that probably both, lipid and ion force field parameters, need improvement to correctly predict the cation binding affinity, and the associated structural changes.

3 Conclusions

As suggested by In accordance with the molecular electrometerconcept [20,29–31], the decrease in [20,29–32], cation binding to lipid bilayers was accompanied with a decrease in the C–H order parameters of α and β carbons in the PC head group of lipids bilayers is related to cation binding in all tested simulation models α and β carbons in all the simulation models tested (Fig. 3) , despite of — despite of the known inaccuracies in the actual atomistic resolution structures[45]. Hence, the molecular electrometer concept allows allowed a direct comparison of Na^+ binding affinity between simulations and non-invasive NMR experiments. The comparison reveals revealed that most models overestimate overestimated Na^+ binding; only Orange, Lipid14, and CHARMM36 predict realistic binding affinitypredicted realistic binding affinities. None of the tested models has the required accuracy had the accuracy required to interpret the Ca^{2+}:lipid stoichiometry or the induced structural changes with atomistic resolution.

In generalTaken together, our results support corroborate the pre-2000 view that at sub-molar concentrations, in contrast to Ca^{2+} and other multivalent ions[1–4,10,11,19,20,27,29], Na^+ and other monovalent ions (except Li^+) do not specifically bind to phospholipid bilayers. Concerning the interpretation of existing experimental data, our work supports Cevc's view[2] that the observed small shift in phase transition temperature is not indicative of Na^+ binding. Further, our findings are in line with the noninvasive NMR spectroscopy work of Filippov et al.[11] that proved the results of Refs. 7,9,12 to be explainable by direct interactions between Na^+ ions and fluorescent probes. Finally, as spectroscopic methods are in general more sensitive to atomistic details in fluid-like environment than AFM, our work indirectly suggests that the ion binding reported from AFM experiments on fluid-like lipid bilayer systems[14–18] might be confounded with other physical features of the system. Concerning contradictions in MD simulation results, we reinterpret the strong Na^+ binding as an artefact of several simulation models, e.g., the Berger model used in Refs. 12,13.

The artificial specific Na^+ binding in MD simulations may lead to doubtful results, since it effectively leads to as it effectively results in a positively charged phosphatidylcholine (PC) lipid bilayers lipid bilayer even at physiological NaCl concentrationconcentrations. Such a PC bilayer has charged bilayer will have distinctly different interactions with charged objects compared to than what a (more realistic) model without specific Na^+ binding would predict. Furthermore, the overestimation of Na^+ binding affinity may extend also from ions to other positively charged objects, say, membrane protein segments. This would affect lipid–protein interactions and could explain, for example, certain contradicting results on electrostatic interactions between charged protein segments and lipid bilayer bilayers [116,117]. In conclusion, more careful studies and model development on lipid bilayer–charged object interactions are urgently called for to make molecular dynamics simulations directly usable in a physiologically relevant electrolytic environment.

This work has been was done as a fully open collaboration, using `nmrlipids.blogspot.fi` as the communication platform. All the scientific contributions have been were communicated publicly through this blog or the GitHub repository[34]. All the related content and data is are available at Ref. 34.

Acknowledgements: AC and VSO wish to thank the Research Computing Service at UEA for access to the High Performance Computing Cluster.—; VSO acknowledges the Engineering and Physical Sciences Research Council in the UK for financial support (EP/L001322/1). OHSO acknowledges Tiago Ferreira for very useful discussions, the Emil Aaltonen foundation for financial support, Aalto Science-IT project and CSC-IT Center for Science for computational resources. MSM acknowledges financial support from the Volkswagen Foundation (86110). M.G. MG acknowledges financial support from Finnish Center of International Mobility (Fellowship TM-9363). J. Melcr acknowledges computational resources provided by the CESNET LM2015042 and the CERIT Scientific Cloud LM2015085 projects under the program "Projects of Large Research, Development, and Innovations Infrastructure". MSM acknowledges financial support from

the Volkswagen Foundation (86110). LM acknowledges funding from the Institut National de la Sante et de la Recherche Medicale (INSERM). OHSO acknowledges Tiago Ferreira for very useful discussions, the Emil Aaltonen foundation for financial support, Aalto Science-IT project and CSC-IT Center for Science for computational resources.

References

1 M. Eisenberg, T. Gresalfi, T. Riccio and S. McLaughlin, *Biochemistry*, 1979, **18**, 5213–5223.

2 G. Cevc, *Biochim. Biophys. Acta - Rev. Biomemb.*, 1990, **1031**, 311 – 382.

3 J.-F. Tocanne and J. Teissié, *Biochim. Biophys. Acta - Reviews on Biomembranes*, 1990, **1031**, 111 – 142.

4 H. Binder and O. Zschörnig, *Chem. Phys. Lipids*, 2002, **115**, 39 – 61.

5 J. J. Garcia-Celma, L. Hatahet, W. Kunz and K. Fendler, *Langmuir*, 2007, **23**, 10074–10080.

6 E. Leontidis and A. Aroti, *J. Phys. Chem. B*, 2009, **113**, 1460–1467.

7 R. Vacha, S. W. I. Siu, M. Petrov, R. A. Böckmann, J. Barucha-Kraszewska, P. Jurkiewicz, M. Hof, M. L. Berkowitz and P. Jungwirth, *J. Phys. Chem. A*, 2009, **113**, 7235–7243.

8 B. Klasczyk, V. Knecht, R. Lipowsky and R. Dimova, *Langmuir*, 2010, **26**, 18951–18958.

9 F. F. Harb and B. Tinland, *Langmuir*, 2013, **29**, 5540–5546.

10 G. Pabst, A. Hodzic, J. Strancar, S. Danner, M. Rappolt and P. Laggner, *Biophys. J.*, 2007, **93**, 2688 – 2696.

11 A. Filippov, G. Orädd and G. Lindblom, *Chem. Phys. Lipids*, 2009, **159**, 81 – 87.

12 R. A. Böckmann, A. Hac, T. Heimburg and H. Grubmüller, *Biophys. J.*, 2003, **85**, 1647 – 1655.

13 R. A. Böckmann and H. Grubmüller, *Ang. Chem. Int. Ed.*, 2004, **43**, 1021–1024.

14 S. Garcia-Manyes, G. Oncins and F. Sanz, *Biophys. J.*, 2005, **89**, 1812 – 1826.

15 S. Garcia-Manyes, G. Oncins and F. Sanz, *Electrochim. Acta*, 2006, **51**, 5029 – 5036.

16 T. Fukuma, M. J. Higgins and S. P. Jarvis, *Phys. Rev. Lett.*, 2007, **98**, 106101.

17 U. Ferber, G. Kaggwa and S. Jarvis, *Eur. Biophys. J.*, 2011, **40**, 329–338.

18 L. Redondo-Morata, G. Oncins and F. Sanz, *Biophys. J.*, 2012, **102**, 66 – 74.

19 R. J. Clarke and C. Lüpfert, *Biophys. J.*, 1999, **76**, 2614 – 2624.

20 H. Akutsu and J. Seelig, *Biochemistry*, 1981, **20**, 7366–7373.

21 J. N. Sachs, H. Nanda, H. I. Petrache and T. B. Woolf, *Biophys. J.*, 2004, **86**, 3772 – 3782.

22 M. L. Berkowitz, D. L. Bostick and S. Pandit, *Chem. Rev.*, 2006, **106**, 1527–1539.

23 A. Cordomí, O. Edholm and J. J. Perez, *J. Phys. Chem. B*, 2008, **112**, 1397–1408.

24 A. Cordomí, O. Edholm and J. J. Perez, *J. Chem. Theory Comput.*, 2009, **5**, 2125–2134.

25 C. Valley, J. Perlmutter, A. Braun and J. Sachs, *J. Membr. Biol.*, 2011, **244**, 35–42.

26 M. L. Berkowitz and R. Vacha, *Acc. Chem. Res.*, 2012, **45**, 74–82.

27 S. A. Tatulian, *Eur. J. Biochem.*, 1987, **170**, 413–420.

28 V. Knecht and B. Klasczyk, *Biophys. J.*, 2013, **104**, 818 – 824.

29 C. Altenbach and J. Seelig, *Biochemistry*, 1984, **23**, 3913–3920.

30 J. Seelig, P. M. MacDonald and P. G. Scherer, *Biochemistry*, 1987, **26**, 7535–7541.

31 P. G. Scherer and J. Seelig, *Biochemistry*, 1989, **28**, 7720–7728.

32 M. F. Brown and J. Seelig, *Nature*, 1977, **269**, 721–723.

33 O. S. Ollila and G. Pabst, *Atomistic resolution structure and dynamics of lipid bilayers in simulations and experiments*, 2016, `http://dx.doi.org/10.1016/j.bbamem.2016.01.019`, In Press.

34 A. Catte, M. Girych, M. Javanainen, C. Loison, J. Melcr, M. S. Miettinen, L. Monticelli, J. Määttä, V. S. Oganesyan, O. H. S. Ollila, J. Tynkkynen and S. Vilov, *lipid_ionINTERACTION: First submission to Physical Chemistry Chemical Physics (PCCP)*, 2016, `http://dx.doi.org/10.5281/zenodo.57845`.

35 C. Altenbach and J. Seelig, *Biochim. Biophys. Acta*, 1985, **818**, 410 – 415.

36 P. M. Macdonald and J. Seelig, *Biochemistry*, 1987, **26**, 1231–1240.

37 M. Roux and M. Bloom, *Biochemistry*, 1990, **29**, 7077–7089.

38 G. Beschiaschvili and J. Seelig, *Biochim. Biophys. Acta - Biomembranes*, 1991, **1061**, 78 – 84.

39 F. M. Marassi and P. M. Macdonald, *Biochemistry*, 1992, **31**, 10031–10036.

40 J. R. Rydall and P. M. Macdonald, *Biochemistry*, 1992, **31**, 1092–1099.

41 T. M. Ferreira, R. Sood, R. Bärenwald, G. Carlström, D. Topgaard, K. Saalwächter, P. K. J. Kinnunen and O. H. S. Ollila, *Langmuir*, 2016, **32**, 6524–6533.

42 M. Hong, K. Schmidt-Rohr and A. Pines, *J. Am. Chem. Soc.*, 1995, **117**, 3310–3311.

43 M. Hong, K. Schmidt-Rohr and D. Nanz, *Biophys. J.*, 1995, **69**, 1939 – 1950.

44 J. D. Gross, D. E. Warschawski and R. G. Griffin, *J. Am. Chem. Soc.*, 1997, **119**, 796–802.

45 A. Botan, F. Favela-Rosales, P. F. J. Fuchs, M. Javanainen, M. Kanduč, W. Kulig, A. Lamberg, C. Loison, A. Lyubartsev, M. S. Miettinen, L. Monticelli, J. Määttä, O. H. S. Ollila, M. Retegan, T. Róg, H. Santuz and J. Tynkkynen, *J. Phys. Chem. B*, 2015, **119**, 15075–15088.

46 J. Seelig, *Cell Biol. Int. Rep.*, 1990, **14**, 353–360.

47 A. A. Gurtovenko, M. Miettinen, , M. Karttunen and I. Vattulainen, *J. Phys. Chem. B*, 2005, **109**, 21126–21134.

48 W. Zhao, A. A. Gurtovenko, I. Vattulainen and M. Karttunen, *J. Phys. Chem. B*, 2012, **116**, 269–276.

This journal is © The Royal Society of Chemistry [year]

49 M. S. Miettinen, A. A. Gurtovenko, I. Vattulainen and M. Karttunen, *J. Phys. Chem. B*, 2009, **113**, 9226–9234.

50 C. M. Franzin, P. M. Macdonald, A. Polozova and F. M. Winnik, *Biochim. Biophys. Acta - Biomembranes*, 1998, **1415**, 219 – 234.

51 S. Ollila, M. T. Hyvönen and I. Vattulainen, *J. Phys. Chem. B*, 2007, **111**, 3139–3150.

52 O. H. S. Ollila, T. Ferreira and D. Topgaard, *MD simulation trajectory and related files for POPC bilayer (Berger model delivered by Tieleman, Gromacs 4.5)*, 2014, {http://dx.doi.org/10.5281/zenodo.13279}.

53 T. P. Straatsma and H. J. C. Berendsen, *J. Chem. Phys*, 1988, **89**, year.

54 O. H. S. Ollila, *MD simulation trajectory and related files for POPC bilayer with 340mM NaCl (Berger model delivered by Tieleman, ffgmx ions, Gromacs 4.5)*, 2015, http://dx.doi.org/10.5281/zenodo.32144.

55 O. H. S. Ollila, *MD simulation trajectory and related files for POPC bilayer with 340mM CaCl_2 (Berger model delivered by Tieleman, ffgmx ions, Gromacs 4.5)*, 2015, http://dx.doi.org/10.5281/zenodo.32173.

56 S.-J. Marrink, O. Berger, P. Tieleman and F. Jähnig, *Biophys. J.*, 1998, **74**, 931 – 943.

57 J. Määttä, *DPPC_Berger*, 2015, http://dx.doi.org/10.5281/zenodo.13934.

58 J. Määttä, *DPPC_Berger_NaCl*, 2015, http://dx.doi.org/10.5281/zenodo.16319.

59 J. Määttä, *DPPC_Berger_NaCl_1Mol*, 2015, http://dx.doi.org/10.5281/zenodo.17210.

60 D. P. Tieleman, J. L. MacCallum, W. L. Ash, C. Kandt, Z. Xu and L. Monticelli, *J. Phys. Condens. Matter*, 2006, **18**, S1221.

61 J. Määttä, *DPPC_Berger_OPLS06*, 2015, http://dx.doi.org/10.5281/zenodo.17237.

62 J. Åqvist, *J. Phys. Chem.*, 1990, **94**, 8021–8024.

63 J. Määttä, *DPPC_Berger_OPLS06_NaCl*, 2015, http://dx.doi.org/10.5281/zenodo.16484.

64 J. Määttä, *DPPC_Berger_OPLS06_NaCl_1Mol*, 2016, http://dx.doi.org/10.5281/zenodo.46152.

65 J. B. Klauda, R. M. Venable, J. A. Freites, J. W. O'Connor, D. J. Tobias, C. Mondragon-Ramirez, I. Vorobyov, A. D. M. Jr and R. W. Pastor, *J. Phys. Chem. B*, 2010, **114**, 7830–7843.

66 H. Santuz, *MD simulation trajectory and related files for POPC bilayer (CHARMM36, Gromacs 4.5)*, 2015, DOI: 10.5281/zenodo.14066.

67 O. H. S. Ollila and M. Miettinen, *MD simulation trajectory and related files for POPC bilayer (CHARMM36, Gromacs 4.5)*, 2015, {http://dx.doi.org/10.5281/zenodo.13944}.

68 R. M. Venable, Y. Luo, K. Gawrisch, B. Roux and R. W. Pastor, *J. Phys. Chem. B*, 2013, **117**, 10183–10192.

69 O. H. S. Ollila, *MD simulation trajectory and related files for POPC bilayer with 350mM NaCl (CHARMM36, Gromacs 4.5)*, 2015, http://dx.doi.org/10.5281/zenodo.32496.

70 O. H. S. Ollila, *MD simulation trajectory and related files for POPC bilayer with 690mM NaCl (CHARMM36, Gromacs 4.5)*, 2015, http://dx.doi.org/10.5281/zenodo.32497.

71 O. H. S. Ollila, *MD simulation trajectory and related files for POPC bilayer with 950mM NaCl (CHARMM36, Gromacs 4.5)*, 2015, http://dx.doi.org/10.5281/zenodo.32498.

72 M. Girych and O. H. S. Ollila, *POPC_CHARMM36_CaCl2_035Mol*, 2015, http://dx.doi.org/10.5281/zenodo.35159.

73 M. Javanainen, *POPC @ 310K, 450 mM of CaCl_2. Charmm36 with default Charmm ions*, 2016, http://dx.doi.org/10.5281/zenodo.51185.

74 M. Girych and O. H. S. Ollila, *POPC_CHARMM36_CaCl2_067Mol*, 2015, http://dx.doi.org/10.5281/zenodo.35160.

75 M. Girych and O. H. S. Ollila, *POPC_CHARMM36_CaCl2_1Mol*, 2015, http://dx.doi.org/10.5281/zenodo.35156.

76 J. Yoo, J. Wilson and A. Aksimentiev, *Biopolymers*, 2016.

77 A. Maciejewski, M. Pasenkiewicz-Gierula, O. Cramariuc, I. Vattulainen and T. Rog, *J. Phys. Chem. B*, 2014, **118**, 4571–4581.

78 M. Javanainen, 2015.

79 M. Javanainen, *POPC @ 310K, varying water-to-lipid ratio. Model by Maciejewski and Rog*, 2014, http://dx.doi.org/10.5281/zenodo.13498.

80 M. Javanainen and J. Tynkkynen, *POPC @ 310K, varying amounts of NaCl. Model by Maciejewski and Rog*, 2015, http://dx.doi.org/10.5281/zenodo.14976.

81 O. H. S. Ollila, J. Määttä and L. Monticelli, *MD simulation trajectory for POPC bilayer (Orange, Gromacs 4.5.)*, 2015, http://dx.doi.org/10.5281/zenodo.34488.

82 O. H. S. Ollila, J. Määttä and L. Monticelli, *MD simulation trajectory for POPC bilayer with 140mM NaCl (Orange, Gromacs 4.5.)*, 2015, http://dx.doi.org/10.5281/zenodo.34491.

83 O. H. S. Ollila, J. Määttä and L. Monticelli, *MD simulation trajectory for POPC bilayer with 510mM NaCl (Orange, Gromacs 4.5.)*, 2015, http://dx.doi.org/10.5281/zenodo.34490.

84 S. Ollila, J. Määttä and L. Monticelli, *MD simulation trajectory for POPC bilayer with 1000mM NaCl (Orange, Gromacs 4.5.)*, 2015, http://dx.doi.org/10.5281/zenodo.34497.

85 O. H. S. Ollila, J. Määttä and L. Monticelli, *MD simulation trajectory for POPC bilayer with 510mM CaCl_2 (Orange, Gromacs 4.5.)*, 2015, http://dx.doi.org/10.5281/zenodo.34498.

86 J. P. M. Jämbeck and A. P. Lyubartsev, *J. Phys. Chem. B*, 2012, **116**, 3164–3179.

87 J. P. M. Jämbeck and A. P. Lyubartsev, *J. Chem. Theory Comput.*, 2012, **8**, 2938–2948.

88 J. Määttä, *DPPC_Slipids*, 2014, http://dx.doi.org/10.5281/zenodo.13287.

89 M. Javanainen, *POPC @ 310K, Slipids force field.*, 2015, DOI:

10.5281/zenodo.13887.
90 D. Beglov and B. Roux, *J. Chem. Phys.*, 1994, **100**, 9050–9063.
91 B. Roux, *Biophys. J.*, 1996, **71**, 3177 – 3185.
92 D. E. Smith and L. X. Dang, *J. Chem. Phys*, 1994, **100**, year.
93 M. Javanainen, *POPC @ 310K, 130 mM of NaCl. Slipids with ions by Smith & Dang*, 2015, http://dx.doi.org/10.5281/zenodo.35275.
94 J. Melcr, *Simulation files for DPPC lipid membrane with Slipids force field for Gromacs MD simulation engine*, 2016, http://dx.doi.org/10.5281/zenodo.55322.
95 M. Javanainen, *POPC @ 310K, 450 mM of CaCl_2. Slipids with default Amber ions*, 2016, http://dx.doi.org/10.5281/zenodo.51182.
96 C. J. Dickson, B. D. Madej, Ã. A. Skjevik, R. M. Betz, K. Teigen, I. R. Gould and R. C. Walker, *J. Chem. Theory Comput.*, 2014, **10**, 865–879.
97 M. Girych and O. H. S. Ollila, *POPC_AMBER_LIPID14_Verlet*, 2015, http://dx.doi.org/10.5281/zenodo.30898.
98 M. Girych and O. H. S. Ollila, *POPC_AMBER_LIPID14_NaCl_015Mol*, 2015, http://dx.doi.org/10.5281/zenodo.30891.
99 M. Girych and O. H. S. Ollila, *POPC_AMBER_LIPID14_NaCl_1Mol*, 2015, http://dx.doi.org/10.5281/zenodo.30865.
100 M. Girych and O. H. S. Ollila, *POPC_AMBER_LIPID14_CaCl2_035Mol*, 2015, http://dx.doi.org/10.5281/zenodo.34415.
101 M. Girych and O. H. S. Ollila, *POPC_AMBER_LIPID14_CaCl2_1Mol*, 2015, http://dx.doi.org/10.5281/zenodo.35074.
102 J. P. Ulmschneider and M. B. Ulmschneider, *J. Chem. Theory Comput.*, 2009, **5**, 1803–1813.
103 M. Girych and O. H. S. Ollila, *POPC_Ulmschneider_OPLS_Verlet_Group*, 2015, http://dx.doi.org/10.5281/zenodo.30904.
104 M. Girych and O. H. S. Ollila, *POPC_Ulmschneider_OPLS_NaCl_015Mol*, 2015, http://dx.doi.org/10.5281/zenodo.30892.
105 M. Girych and O. H. S. Ollila, *POPC_Ulmschneider_OPLS_NaCl_1Mol*, 2015, http://dx.doi.org/10.5281/zenodo.30894.
106 H. Hauser, M. C. Phillips, B. Levine and R. Williams, *Nature*, 1976, **261**, 390 – 394.
107 H. Hauser, W. Guyer, B. Levine, P. Skrabal and R. Williams, *Biochim. Biophys. Acta - Biomembranes*, 1978, **508**, 450 – 463.
108 L. Herbette, C. Napolitano and R. McDaniel, *Biophys. J.*, 1984, **46**, 677 – 685.
109 B. Hess, C. Holm and N. van der Vegt, *J. Chem. Phys*, 2006, **124**, year.
110 A. A. Chen, and R. V. Pappu, *J. Phys. Chem. B*, 2007, **111**, 11884–11887.
111 M. M. Reif, M. Winger and C. Oostenbrink, *J. Chem. Theory Comput.*, 2013, **9**, 1247–1264.
112 I. Leontyev and A. Stuchebrukhov, *Phys. Chem. Chem. Phys.*, 2011, **13**, 2613–2626.
113 W. L. Jorgensen, D. S. Maxwell and J. Tirado-Rives, *J. Am. Chem. Soc.*, 1996, **118**, 11225–11236.
114 M. Kohagen, P. E. Mason and P. Jungwirth, *J. Phys. Chem. B*, 2016, **120**, 1454–1460.
115 M. Kohagen, P. E. Mason and P. Jungwirth, *J. Phys. Chem. B*, 2014, **118**, 7902–7909.
116 A. Arkhipov, Y. Shan, R. Das, N. Endres, M. Eastwood, D. Wemmer, J. Kuriyan and D. Shaw, *Cell*, 2013, **152**, 557 – 569.
117 K. Kaszuba, M. Grzybek, A. Orlowski, R. Danne, T. Róg, K. Simons, Ã. Coskun and I. Vattulainen, *Proc. Natl. Acad. Sci. USA*, 2015, **112**, 4334–4339.

This journal is © The Royal Society of Chemistry [year]

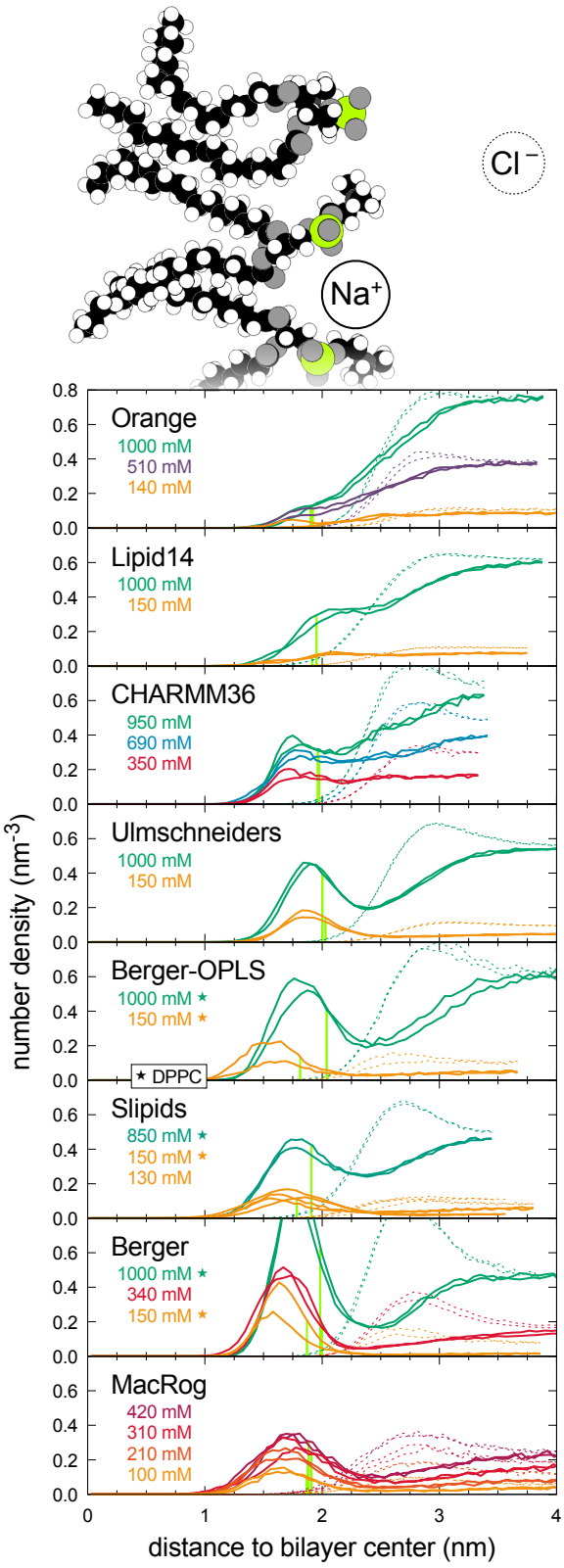

Fig. 4 Na^+ (solid line) and Cl^- (dashed) distributions along the lipid bilayer normal from MD simulations at several NaCl concentrations. The eight MD models are ordered according to their strength of order parameter change in response to NaCl (Fig. 2) from the weakest (top panel) to the strongest (bottom). The light green vertical lines indicate the locations of the Phosphorus maxima, used to define bound cations in Fig. 3.

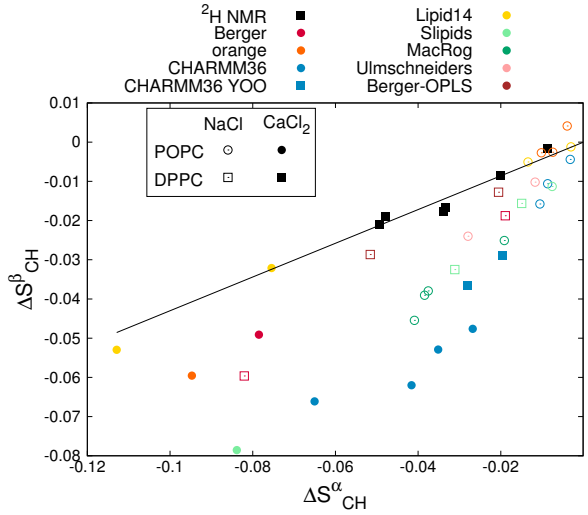

Fig. 5 Relation between ΔS^{β}_{CH} and ΔS^{α}_{CH} from experiments[20] and different simulation models. Solid line is $\Delta S^{\beta}_{CH} = 0.43 \Delta S^{\alpha}_{CH}$ determined for DPPC bilayer from ^{2}H NMR experiment with various $CaCl_2$ concentrations[20].

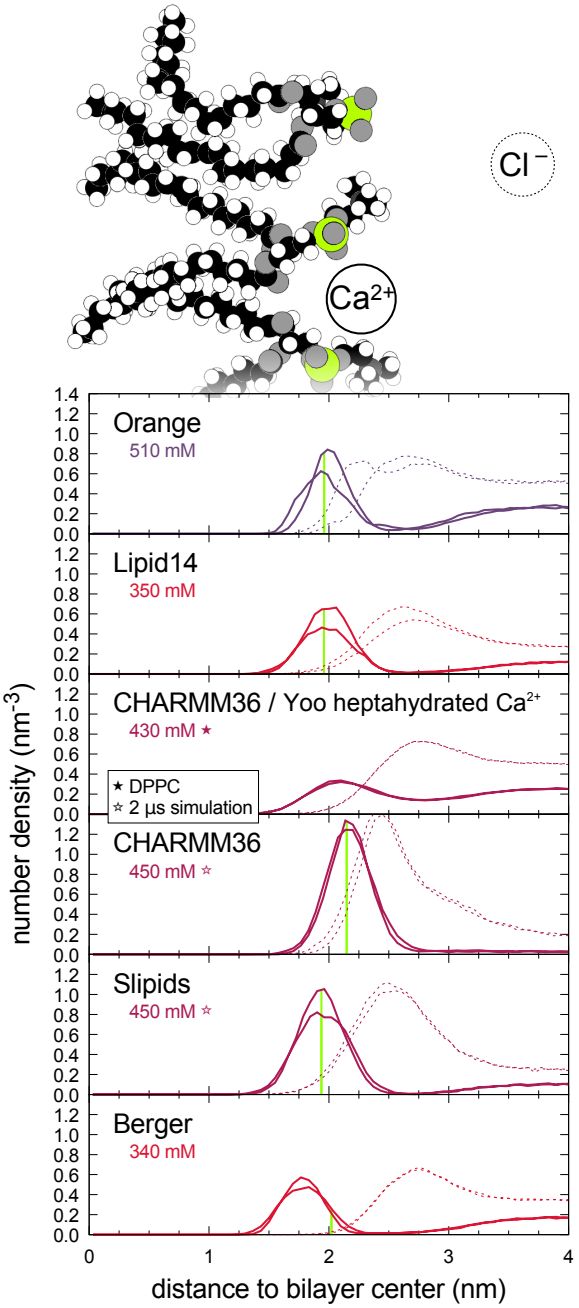

Fig. 6 ~~Atom number density profiles along the membrane normal coordinate z for lipids,~~ Ca^{2+} (solid line) and Cl^- ~~ions~~ (dashed) distributions along the lipid bilayer normal from MD simulations~~with different force fields~~. ~~The profiles~~ For clarity, only ~~with smallest available~~ one $CaCl_2$ concentration ~~are~~ per MD model is shown; see ESI† for ~~clarity. Figure~~ a plot including all the available concentrations~~is shown in ESI†~~. The ~~lipid densities are scaled with 100 (united atom) or 200 (all atom model) to make them visible with~~ light green vertical lines indicate the locations of the Phosphorus maxima, used ~~y-axis scale. The Cl^- density is scaled with 2~~ to ~~equalise charge density of ions~~define bound cations in Fig. 3.

This journal is © The Royal Society of Chemistry [year]